Provided for non-commercial research and education use.
Not for reproduction, distribution or commercial use.

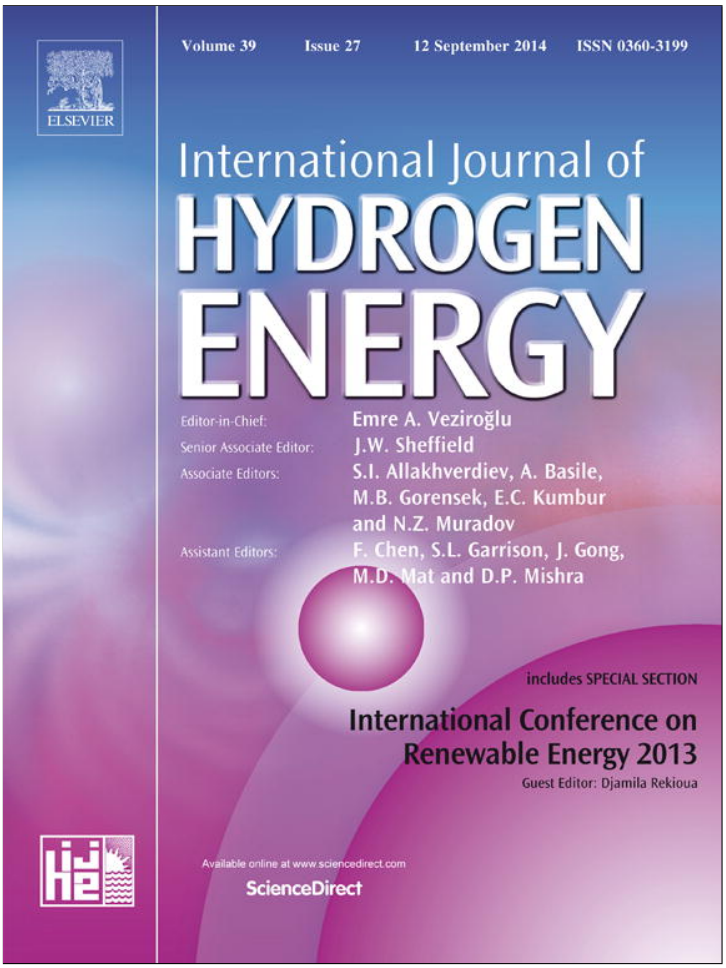

This article appeared in a journal published by Elsevier. The attached copy is furnished to the author for internal non-commercial research and education use, including for instruction at the authors institution and sharing with colleagues.

Other uses, including reproduction and distribution, or selling or licensing copies, or posting to personal, institutional or third party websites are prohibited.

In most cases authors are permitted to post their version of the article (e.g. in Word or Tex form) to their personal website or institutional repository. Authors requiring further information regarding Elsevier's archiving and manuscript policies are encouraged to visit:

http://www.elsevier.com/authorsrights

Author's personal copy

INTERNATIONAL JOURNAL OF HYDROGEN ENERGY 39 (2014) 14834–14842

Available online at www.sciencedirect.com

ScienceDirect

journal homepage: www.elsevier.com/locate/he

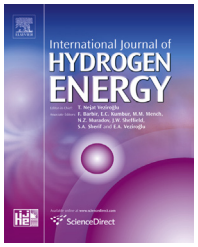

Interaction mechanism of hydrogen storage materials with layer-by-layer applied protective polyelectrolyte coatings

Georgia Sourkouni [a], *Florian Voigts* [b], *Jan C. Namyslo* [c], *Sebastian Dahle* [b], *Wolfgang Maus-Friedrichs* [b], *Christos Argirusis* [d,*]

[a] *Institut für Elektrische Energietechnik, Clausthal University of Technology, Leibnizstr. 28, 38678 Clausthal-Zellerfeld, Germany*

[b] *Institut für Energieforschung und Physikalische Technologien, Clausthal University of Technology, Leibnizstr. 4, 38678 Clausthal-Zellerfeld, Germany*

[c] *Institut für Organische Chemie, Clausthal University of Technology, Leibnizstr. 6, 38678 Clausthal-Zellerfeld, Germany*

[d] *School of Chemical Engineering, National Technical University of Athens, Zografou 15780, Athens, Greece*

ARTICLE INFO

Article history:
Received 5 April 2014
Received in revised form
22 June 2014
Accepted 23 June 2014
Available online 2 August 2014

Keywords:
Hydrogen storage materials
Metal hydrides
Polyelectrolytes
Layer-by-layer protective coatings
Sodium borohydride

ABSTRACT

Metal hydrides are promising compounds for the storage of hydrogen especially in the transport sector. Their high reactivity with moisture and difficult handling in ambient atmosphere prevents their easy application in tanks and thus the market penetration of this very promising and clean technology. In the present work we investigated the way to protect sodium borohydride with organic polyelectrolytes like polyethyleneimine (PEI) and dicarboxy terminated poly(acrylonitrile-co-butadiene-co-acrylic acid) (PABA) with emphasis on the interaction of those polyelectrolytes with the SBH. The polyelectrolytes protect SBH either by electrostatic adsorption or by reacting with it, depending on the reactive groups present in their structure. PABA undergoes only an electrostatic interaction with the SBH substrate. PEI on the other hand interacts chemically with the SBH substrate and forms complexes with groups on the SBH surface. Both polyelectrolytes can be applied in a layer-by-layer approach on the SBH in order to protect it. Regarding the best order of the layer application XPS results yield that the formation of the boron-amino-complexes between the PEI and the SBH is independent of the order in which the PABA and PEI layers are applied. However, the rearrangement of the SBH surface groups due to the application of the PEI films has been found to be considerably influenced by the order of application. The effect of a PEI film has been mostly compensated by the subsequent application of a PABA film, while the application of PEI had a much larger influence on the surface of a PABA coated SBH sample. Thus, the best order of the layer application with respect to the application according to XPS is to deposit the PEI layer at first and the PABA layer afterwards.

Copyright © 2014, Hydrogen Energy Publications, LLC. Published by Elsevier Ltd. All rights reserved.

* *Corresponding author.*
E-mail address: amca@chemeng.ntua.gr (C. Argirusis).

http://dx.doi.org/10.1016/j.ijhydene.2014.06.124

0360-3199/Copyright © 2014, Hydrogen Energy Publications, LLC. Published by Elsevier Ltd. All rights reserved.

Author's personal copy

Introduction

The prospective sources of chemical energy for a variety of applications will most probably be based on hydrogen [1,2] and it is expected that hydrogen will play the key role especially in the transport area. The storage of hydrogen though remains as one of the most critical tasks prior to establish a hydrogen economy and it still has not been overcome [2].

The difficulties in storing hydrogen originate from its low density and low critical temperature. On one hand, there are different physical approaches for hydrogen storage that are currently investigated, including compressed or liquefied hydrogen in tanks [1], adsorption on activated carbon [3,4] and carbon nanotubes [4,5], hydrogen-absorbing alloys [5], or metal-organic frameworks [6].

On the other hand, different chemical storage methods and materials are being explored, such as inorganic hydrides including simple metal hydrides as NaH [7], LiH [6] or MgH_2 [8] as well as alanates like $NaAlH_4$ [9] or metal borohydrides as $LiBH_4$ [10] and $NaBH_4$ [5,11]. Furthermore, some approaches use amides [6] or organic hydrogen-enriched compounds (methylcyclohexane, decalin) [12,13].

A decreased grain size of such complex metal hydrides, structural defects introduced via ball-milling and especially the addition of nanometric elemental metals have been found to enhance the hydrogen desorption rates significantly [14,15].

The hydrogen content of complex metal hydrides is most commonly released by hydrolysis [16], while it is also possible to reversely release the hydrogen via thermal desorption [17].

The complex metal hydrides exhibit a much easier handling than the other storage approaches. Amongst these complex metal hydrides, the $NaBH_4$ is considered to be the most attractive hydride for its easy synthesis [2]. However, all of these materials suffer from severe ageing after long times of exposure to air or other humid environments by forming surface oxides which act as kinetic barriers for hydrogen desorption [18]. In many cases it is even not possible to work with those materials in ambient atmosphere. Thus, the complex metal hydrides as hydrogen storage materials have to be protected from direct contact with the surrounding atmosphere making possible their easy and safe handling for long time, for example during packaging of these materials in storage tanks and devices. This protection can be done e.g. via interfacial polymer precipitation induced by solvent evaporation. Sodium boron hydride has been successfully protected for example with a polystyrene shell by co-precipitation. This shell provides a hydrophobic barrier for water diffusion into the container interior [19]. Furthermore, multiple polyelectrolytes can be employed to build up the protecting shell from alternating anionic and cationic polyelectrolytes. For best results, these shell materials have to be water impermeable but H_2 permeable.

In the present study we used alternating polyelectrolyte layers of polyethyleneimine (PEI) and dicarboxy terminated poly(acrylonitrile-co-butadiene-co-acrylic acid) (PABA) as protecting shell (see Fig. 1) and investigated its influence on the stability of sodium borohydride (SBH). Thus, we extend the preliminary results on the thermal stability and the hydrogen release of SBH protected by polyelectrolyte shells [17], where

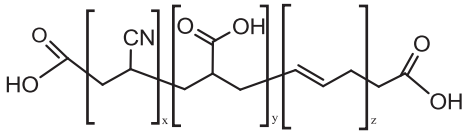

Poly(acrylonitrile-co-butadiene-co-acrylic acid), dicarboxy terminnated: PABA [M ~ 3.600 g/mol]

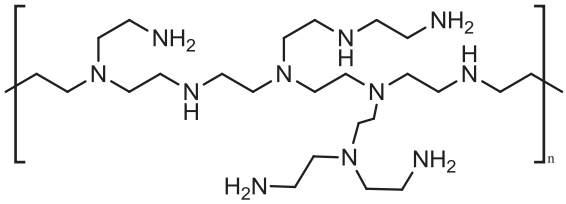

Polyethylenimine, branched:PEI [M ~ 10,000 g/mol]

Fig. 1 – Chemical formulae of the used polyelectrolytes PEI and PABA.

we found both polyelectrolytes to enhance the hydrogen release. This was found to be most significant for PEI, which also effectively lowered the hydrogen release temperature. The PABA coating slightly increased the hydrogen release temperature, but improved the stability of the SBH substrate as well.

As reported in the literature [2,20], the layer-by-layer method effectively protects sensitive hydrogen storage materials like SBH. PABA and PEI form stable complexes with SBH and the formed shell is impermeable to polar compounds like water, thus effectively protecting the hydrogen storage material. In doing so, ζ-potential measurements revealed an electrostatic interaction between PABA and SBH leading to very stable films, while PEI would not directly stick to the SBH by electrostatic interactions [2].

A previous study proved the formation of stable films of PABA as well as PEI on SBH. These films appeared to completely cover the surface of the SBH grains, while exhibiting a rough surface structure [17]. However, these works have shown the protection of the hydrogen storage material in a more or less empirical way. In the course of the present work, the interaction of the polyelectrolytes with SBH as well as with each other when they are applied on SBH in an alternating way has been investigated by means of X-ray photoelectron spectroscopy (XPS), nuclear magnetic resonance spectroscopy (NMR), and Fourier transform infrared spectroscopy (FT-IR).

Results

In the following sections we present results obtained from measurements on the used materials performed by means of the experimental methods presented in the experimental section.

Author's personal copy

XPS

Fig. 2 shows the XPS detail spectra of the B 1s regions of pure SBH (A, top left section), SBH after dichloromethane (DCM) treatment, i.e. after washing each sample twice with dichloromethane as described in Sect. 5 (B, top right section), SBH after adsorption of PABA (C, middle left section), SBH after adsorption of PEI (D, middle right section), SBH after consecutive adsorption of PEI and PABA (E, bottom left section) and SBH after consecutive adsorption of PABA and PEI (F, bottom right section). The original data are displayed as black squares, while the sum of the peak fit is shown as solid red line. Two different chemical components are found for all B 1s spectra, the corresponding Gaussians are drawn as green lines.

The XPS B 1s peak corresponding to SBH has been reported to be found at 187.4 eV [21,22]. The main features (I) of the spectra presented in Fig. 2 are all shifted towards higher binding energies due to homogeneous electrical charging of the powder samples. The second chemical component within the B 1s region (II) most probably belongs to different molecules chemisorbed at the surface of the sodium borohydride particles.

In Fig. 3, sodium to boron ratios and XPS Boron 1s peak ratios for SBH before and after adsorption of DCM, PABA or PEI, as well as SBH after consecutive adsorption of PEI and PABA or PABA and PEI are plotted.

The second boron state B 1s:A_{II} represents boron bonds other than within the SBH. For the pure SBH, these are most probably related to adsorbates from the production of the SBH powder. A similar value for the DCM treated as well as the PABA coated samples indicate the absence of chemical interactions between the SBH and the solvent or polyelectrolyte, respectively. The adsorption of PEI however leads to an increase of this second state by one third revealing a chemical interaction between the PEI and the SBH, i.e. a formation of bonds between the BH_4-group of the SBH and the PEI. Both bilayer samples yielded the formation of twice as much bonds compared to the sole adsorption of PEI.

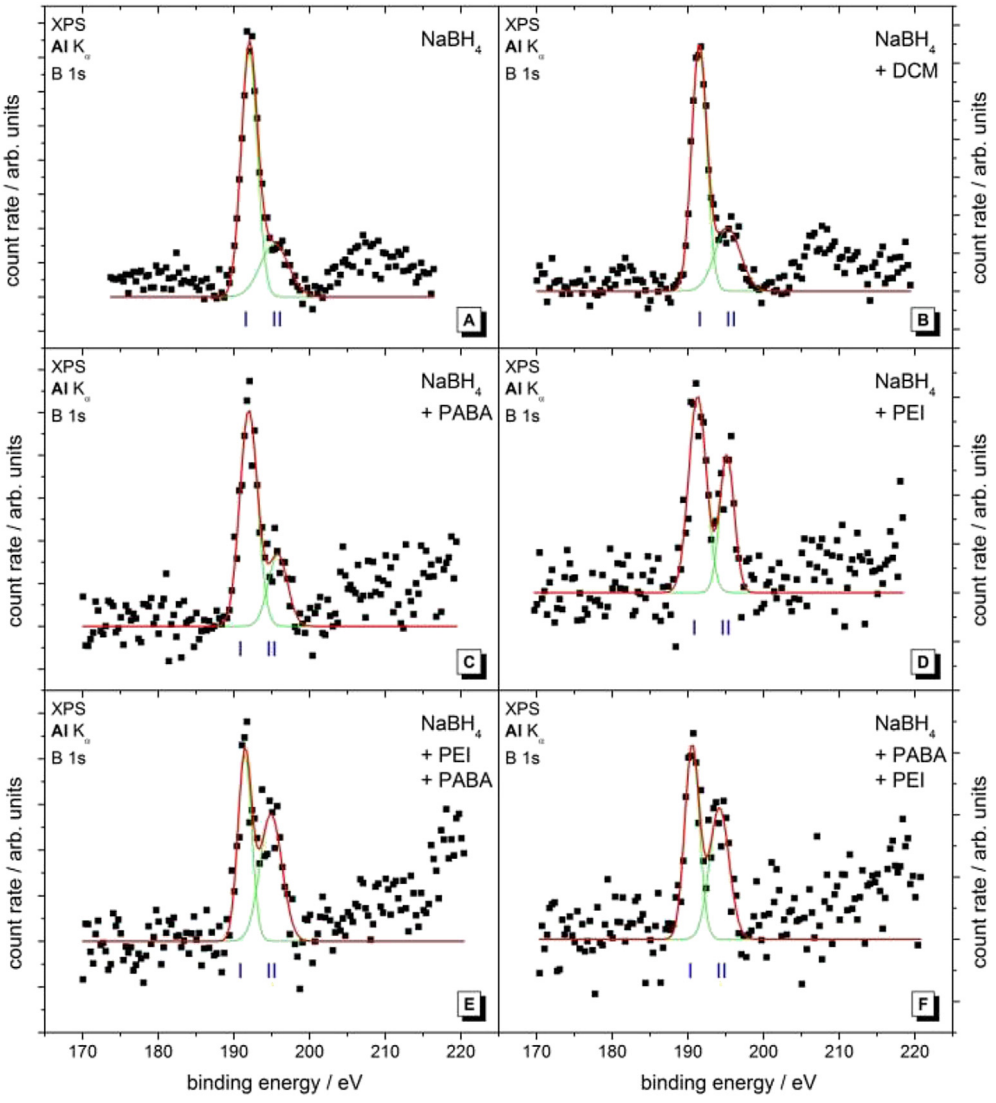

Fig. 2 – XPS detail spectra of the B 1s region of SBH before (A) and after adsorption of DCM (B), PABA (C) or PEI (D), as well as SBH after consecutive adsorption of PEI and PABA (E) or PABA and PEI (F).

Author's personal copy

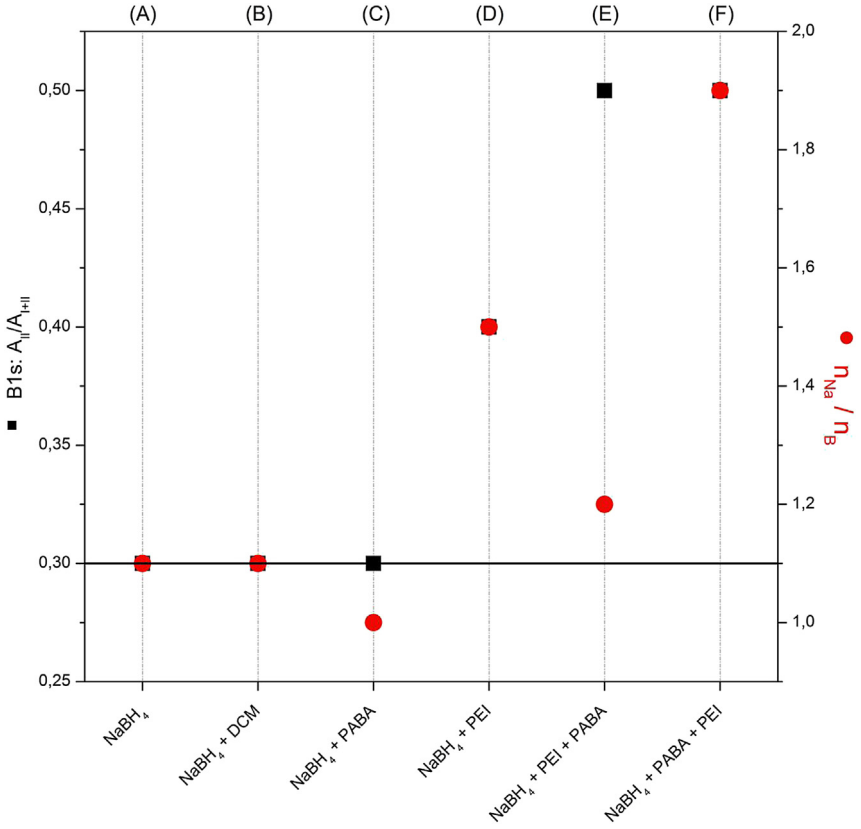

Fig. 3 – Sodium to boron ratios (red circles) and XPS B 1s peak ratios (black squares) for SBH before (A) and after adsorption of DCM (B), PABA (C) or PEI (D), as well as after consecutive adsorption of PEI and PABA (E) or PABA and PEI (F). (For interpretation of the references to colour in this figure legend, the reader is referred to the web version of this article.)

The sodium to boron ratios have been evaluated from the XPS stoichiometries, yielding a value of 1.1 for the pristine SBH. This might be a structural effect due to a mainly sodium-terminated surface of the SBH or a surface complexation where BH_4-groups are replaced via the chemisorption of molecules from the production process. This ratio does not get influenced by the DCM treatment. After the adsorption of PABA, a slightly decreased value of 1.0 was found, which is most probably due to the Coulomb interactions between the positively charged PABA and the tetrahydroborate anions mediating the physisorption. This might be the reason for the enhanced reaction of PEI with the PABA precoated SBH samples as shown above. The adsorption of a PEI led to an increase up to 1.5, while the additional adsorption of a PABA layer onto the PEI coated SBH reduced the ratio to 1.2. This might indicate the structural effect to be a reversible process where the adsorption of PABA induces a diffusion of unreacted $(BH_4)^-$ – groups towards the surface or the diffusion of leftover sodium cations into the bulk. Thereagainst, the adsorption of PEI onto a PABA precoated SBH sample led to a ratio of 1.9, indicating a structural influence twice as big as for the single PEI layer. This enhancement of the reaction of PEI with the tetrahydroborate groups at the SBH surface by the Coulomb interaction of physisorbed PABA might be a simple geometrical effect, i.e. increasing the number of accessible adsorption sites for the PEI.

Thus the formation of the boron-amino-complexes between the PEI and the SBH as represented by the B 1s:A_{II} fraction (c.f. black squares in Fig. 3) is independent of the order in which the PABA and PEI layers are applied. On the other hand, the rearrangement of the SBH surface groups due to the application of the PEI films has been found to be considerably influenced by the order of application, as indicated by the Na/B ratio (c.f. red circles in Fig. 3).

NMR

According to Fig. 4, which shows a stacked plot of virtually identical 1D carbon spectra of fresh PABA (blue) and PABA after contact with SBH (red), no NMR spectroscopic change of the PABA resonances was to observe upon exposure of PABA to sodium borohydride. From that, it has to be concluded that no durable interaction occurs after initial contact of both of these compounds. As a control experiment, a proton NMR was measured to retest the initially unexpected absence of SBH. Indeed, no borohydride resonance lines where found that could evidence the formation of a PABA/SBH complex.

In contrast to application of PABA, comparison of 1D carbon spectra of fresh PEI and PEI after contact with SBH unambiguously resulted in different spectral appearance (Fig. 5).

Author's personal copy

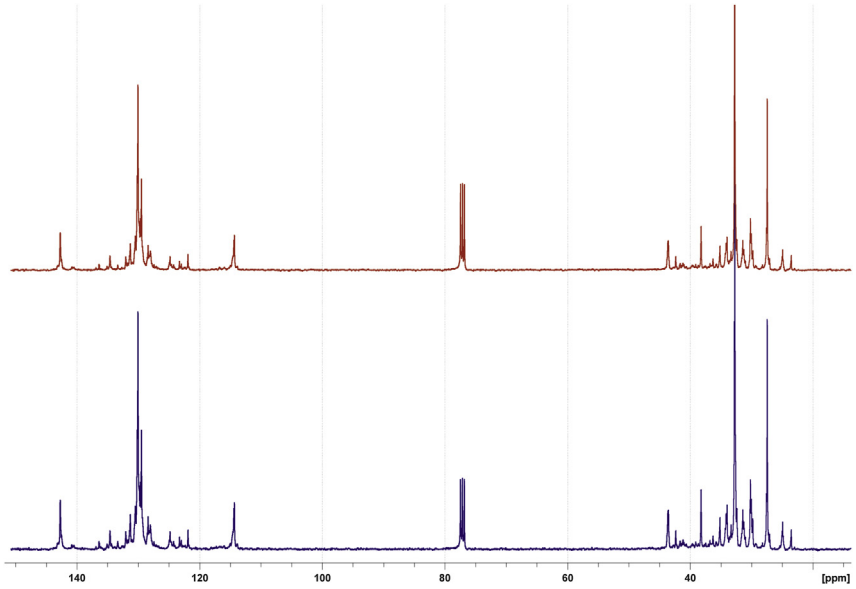

Fig. 4 – $^{13}C\{^1H\}$ comparison of fresh PABA (blue) and PABA after contact with SBH (red). (For interpretation of the references to colour in this figure legend, the reader is referred to the web version of this article.)

Due to substantial overlap of the broad signals caused by the polymeric nature of these analytes, detailed structural assignment based on these 1D spectra was precluded. To circumvent these difficulties, both samples were compared by means of their corresponding 2D-^1H,^{13}C-HMBC spectra (Fig. 6).

The black arrow marks the cross signal (group of almost identical cross signals) which is (are) caused by methylene carbon atoms of terminal free amine side chains $H_2N{-}\underline{C}H_2{-}CH_2{-}NR_2$ ($R \neq H$) of PEI (c.f. Fig. 4). The corresponding carbon shift is the most shielded one (about 38 ppm chemical shift), which allows for assignment to a primary amine. However, carbon atoms in α-position to secondary or tertiary amine groups are found at least about 10 ppm more deshielded. The disappearance of this primary amine cross signal upon treatment with SBH proves the strong interaction of the hydride particularly with the aforementioned primary amino position. Moreover, significant changes in the signal pattern for the cross peaks within and/or more adjacent to the polymeric backbone (carbon nmr region from about 47 to 57 ppm) clearly reveal additional influence of SBH. In this context, the red arrow in Fig. 6 marks the α-methylene carbon of a side chain that structurally ends up with a bis(aminoethyl)amino unit, i.e. $R{-}N(CH_2CH_2NH_2)_2$. All these assignments are in agreement with literature data for amine shifts [23] and with carbon chemical shift prediction using current ACD labs NMR prediction software [24].

FT-IR

In Fig. 7 we present FT-IR spectra of the polyelectrolyte PEI before and after 15 min contact with SBH. It is obvious that the spectrum contains a new band at 2230 cm^{-1} corresponding to

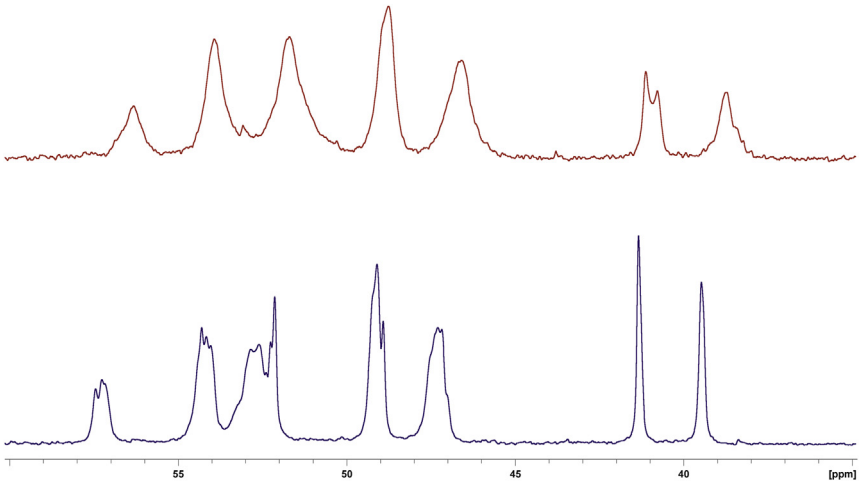

Fig. 5 – $^{13}C\{^1H\}$ comparison of fresh PEI (blue) and PEI after contact with SBH (red). (For interpretation of the references to colour in this figure legend, the reader is referred to the web version of this article.)

Author's personal copy

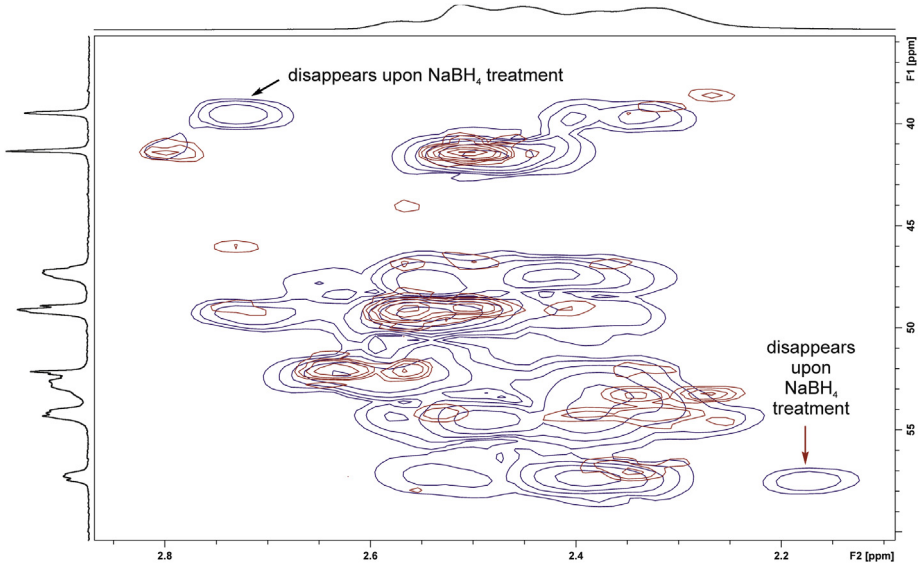

Fig. 6 – Comparison of the HMBC-signals of fresh PEI (blue) and PEI after contact with SBH (red).

B–H stretching vibrations of the complexing borohydride. This wave number is in accordance with the literature [25] and was verified by own DFT calculations applying the current Spartan computational software [26] using the implemented BP (Becke-Perdew) [27,28] density functional and 6-311 + G** basis set. At the same time the band at 3292 cm^{-1} which corresponds to $-NH_2$ disappears.

Discussion

The ζ-potential of the SBH surface as reported in the literature predicts an electrostatic adsorption of the PABA polyelectrolyte on the SBH surface, while the PEI electrolyte should not adsorb steadily [2]. The experimental results however contradicted this presumption, yielding the formation of stable films of PEI on SBH as well as PABA on SBH.

In XPS (Fig. 2), the B 1s detail spectra clearly indicate chemical interaction only between the PEI and the SBH. We found a drastic change in the Na/B ratio (Fig. 2) indicating a significant rearrangement of the SBH surface groups at the interface between SBH and PEI because of the interaction with PEI. Higher Na/B ratios indicate lower densities of tetrahydroborate groups at the surface and thus longer distances for heat conduction and gas diffusion upon hydrogen release. Thus, the samples with lower Na/B ratios should presumably be preferable regarding the application. In fact, the results show the exact opposite, i.e. in comparison to the pristine SBH, the hydrogen release temperature increased for the PABA coated SBH, whereas it decreased for the PEI coated SBH. Thus, the Coulomb interactions with PABA adsorbates seem to stabilize the BH_4-groups, while the formation of boron-amino-complex at the PEI coated SBH reduces the temperature necessary for decomposition. The binding energy of the main B 1s state corresponding to BH_x groups is similar to the binding energy of amorphous boron. The second boron state in comparison is within a range, where B–C- and B–O-bonds can be excluded. The only known bonds resulting in similar binding energies are B–Ph-, B–Cl-, B–N- or complex boron-amide-groups.[22] Thus, the initial fraction of the second boron state should represent residuals from the production process, which are mainly chlorine anions according to the manufacturer. The PEI molecule contains many functional NH- and NH_2-groups (c.f. Fig. 1), thus giving many opportunities for the formation of B–N-bonds. The PABA molecule on the contrary does only contain few very stable CN-groups, which are unlikely to form B–N-bonds. This behaviour is also confirmed for multilayer systems from PABA and PEI upon SBH. Furthermore, the NMR results (see below) strongly support these results. The change in the sodium to boron ratios for all coated SBH samples including PEI layers indicates a significant restructuring of the SBH particles' surfaces upon the reaction between the PEI and the SBH. The formation of the boron-amino-complexes between the PEI and the SBH as represented by the B 1s:A_{II} fraction (c.f. black squares in Fig. 3) is independent of the order in which the PABA and PEI layers are applied. However, the rearrangement of the SBH surface groups due to the application of the PEI films has been found to be considerably influenced by the order of application, as indicated by the Na/B ratio (c.f. red circles in Fig. 3). Evidently, the effect of structural rearrangement of the SBH surface due to a PEI film, i.e. an increase of Na/B from 1.1 to 1.5 (c.f. Fig. 3(A and D)), has been mostly compensated by the subsequent application of a PABA film (c.f. Fig. 3(E)), while the application of PEI had an influence on the surface of a PABA coated SBH sample twice as large as on the pristine SBH surface (c.f. Fig. 3(D and F)). However, the exact nature of this presumptive structural rearrangement is yet unclear.

Similar to XPS, NMR measurements have shown that PABA does not interact at all chemically with the SBH. The protective layer of PABA on SBH is of pure electrostatic nature which is logical taking into account the positive ζ-potential of SBH and

Author's personal copy

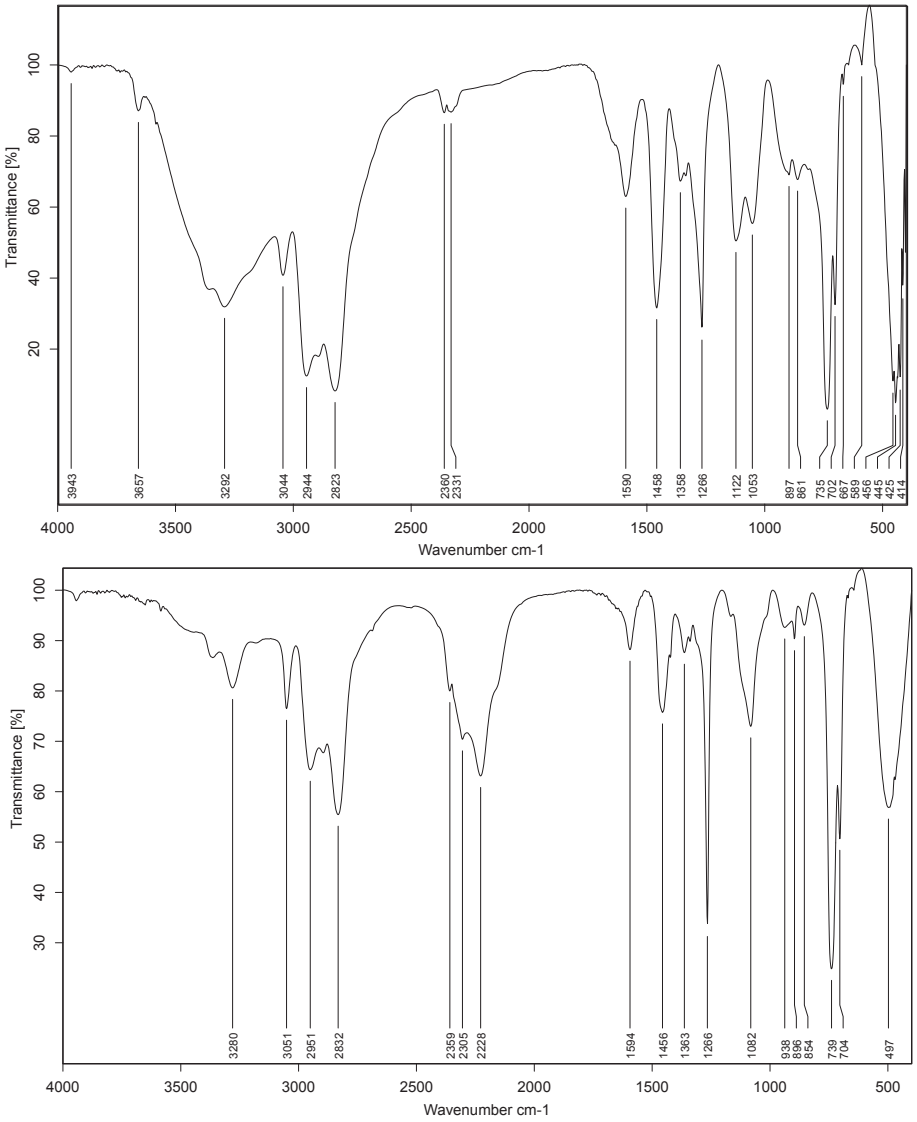

Fig. 7 – IR spectra of PEI (top) and PEI after contact with SBH (bottom).

the negative one of PABA as reported by e.g. Borodina et al. [2]. PEI on the other hand exhibits clearly different spectral appearance, especially of methylene carbon atoms in α-position to terminal amino groups which are the most accessible functionalities of PEI for interaction with SBH. Similarly, significant chemical shift differences that occur upon interaction of SBH with PEI are found for carbon atoms adjacent to further primary or secondary amino substituents. This behaviour clearly indicates remarkable changes of the electron distribution within these amino moieties of the branched part of PEI caused by strong interaction with the applied borohydride.

The FT-IR results of the polyelectrolyte PEI before and after only 15 min contact with SBH show that the spectrum contains a new band at 2230 cm^{-1} corresponding to B–H stretching vibrations of the complexing borohydride. At the same time the band at 3292 cm^{-1} which corresponds to $-NH_2$ disappears. A strong B–N complexation or even a B–N bond formation is probably evidenced by significant IR spectroscopic changes around 1100 cm^{-1}. This assumption is also supported by calculations of a hypothetic fragment (R)–CH_2–NH_2–BH_3 based on the abovementioned DFT parameters. This is another confirmation of the XPS and NMR findings, namely that PEI directly reacts with SBH forming complexes over the amino groups. Based on the results discussed up to now we suggest the formation of a complex between PEI and SBH.

PABA forms as well a protective layer on the SBH substrate which is of pure electrostatic nature. The coverage of the SBH surface by PABA is high and it acts both as a catalyst for hydrogen release as well as strong protection against increased temperatures [17]. On the other hand when PEI is applied after PABA in order to form protective multilayers the interaction of PEI is as if PABA is not present. That means that the PABA layer is either porous (pores must be smaller than 1 μm because they are not detectable by means of confocal laser microscopy) [17] or PEI dissolves PABA partly upon application and penetrates through it in order to form the complex shown in Fig. 8 as confirmed by XPS and NMR.

Author's personal copy

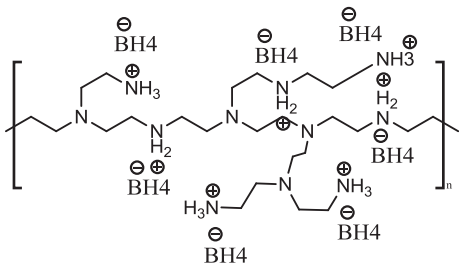

Fig. 8 – Proposed complex formed between the SBH substrate and the protective PEI layer.

Conclusion

We have shown that organic polyelectrolytes protect SBH either by electrostatic adsorption but also by reacting with it, depending on the reactive groups present in their structure. PABA undergoes only an electrostatic interaction with the SBH substrate. PEI on the other hand interacts chemically with the SBH substrate and forms complexes whose structure, despite the findings in the present work, has to be confirmed in future work for example by means of neutron diffraction.

Both polyelectrolytes can be applied in a layer-by-layer approach on the SBH in order to protect it. Regarding the best order of the layer application which is normally determined by the ζ-potential of the SBH surface, in the present case the XPS results yield that the formation of the boron-amino-complexes between the PEI and the SBH is independent of the order in which the PABA and PEI layers are applied. However, the rearrangement of the SBH surface groups due to the application of the PEI films has been found to be considerably influenced by the order of application. The effect of a PEI film has been mostly compensated by the subsequent application of a PABA film, while the application of PEI had a much larger influence on the surface of a PABA coated SBH sample. Thus, the best order of the layer application with respect to the application according to XPS is to deposit the PEI layer at first and the PABA layer afterwards.

In summary, the two electrolytes PABA and PEI adsorbed very strongly on the SBH surface by electrostatical and chemical interactions, respectively, as well as a significant effect of rearrangement on the SBH. The nature and strength of these bonds (q.v. Dahle et al. [17]) gives evidence that these films act as protective agents against decomposition by water as well as mechanical damages as already reported [2]. Furthermore, they allow a future SBH based storage device to be operated at lower temperatures and yet higher hydrogen release rates. Thus, the application of polyelectrolytes as protective layers is a viable way to improve the safety in handling of hydrogen storage materials towards a strong hydrogen economy.

Experimental section

X-ray photoelectron spectroscopy (XPS)

XPS is carried out at room temperature in an ultra-high vacuum apparatus with a base pressure of 5×10^{-11} hPa described elsewhere [29], using a hemispherical analyzer (VSW HA100) and a commercial non-monochromatic X-ray source (Specs RQ20/38C). During XPS, X-ray photons irradiate the surface under an angle of 80° to the surface normal, illuminating a spot with a diameter of several mm. For all measurements presented here the Al K_α line (photon energy 1486.6 eV) is used. Electrons are recorded by the hemispherical analyzer with an energy resolution of 1.1 eV emitted under an angle of 10° to the surface normal. All XPS spectra are displayed as a function of binding energy with respect to the Fermi level.

For quantitative XPS analysis, photoelectron peak areas are calculated via mathematical fitting with Gauss-type profiles using OriginPro 7G including the PFM fitting module, which applies Levenberg–Marquardt algorithms to achieve the best agreement possible between experimental data and fit. A linear background correction, photoelectric cross sections as calculated by Scofield [30], and inelastic mean free paths from the NIST database [31] as well as the energy dependent transmission function of our hemispherical analyzer are taken into account when calculating the stoichiometry.

Nuclear magnetic resonance (NMR)

Solution state NMR measurements were performed on a 9.4 T FT-NMR spectrometer BRUKER Avance with 400 MHz proton frequency equipped with a BBO probehead (Bruker-Biospin, Rheinstetten, Germany). All measurements were carried out at room temperature in deuterated chloroform 99.6% (purchased from Deutero GmbH, Kastellaun, Germany). Proton spectra were referenced to the residual solvent peak at 7.26 ppm chemical shift, whereas in case of proton-decoupled carbon spectra, $^{13}C\{^1H\}$, the solvent signal was set to 77.0 ppm.

In addition to standard one-dimensional NMR spectra, gradient-selected heteronuclear multiple bond correlations (gs-2D-^{1}H,^{13}C-HMBC) were measured in case of fresh PEI and PEI after treatment with SBH.

Infrared spectroscopy (FT-IR)

Infrared spectroscopy (FT-IR) measurements were performed on a BRUKER-IR Vector 22 spectrometer. All measurements were carried out at room temperature by applying the polyelectrolyte before and after contact with SBH between two NaCl plates. Spectra were recorded between 400 and 4000 cm^{-1}.

Sample preparation

The protective coatings have been applied to the sodium borohydride (Sigma–Aldrich purum p.a., ≥96%) via the layer-by-layer approach first reported by Decher et al. [20], using the adapted procedure for organic solvents as developed by Dobbins et al. [32] and Borodina et al. [2,19] Thus, for each layer 16 mg of the corresponding polyelectrolyte (PABA or PEI) has been dissolved in 4 ml of dichloromethane (DCM). After 200 mg of the micrometer sized SBH were incubated in this solution for 5 min, the polyelectrolyte solution has been decanted. The remaining SBH was filtrated and washed two times with 4 ml of DCM in order to remove loose-packed residuals of

Author's personal copy

the polyelectrolyte, before the prepared SBH was dried overnight in a desiccator over $CaCl_2$.

Acknowledgements

Financial support for travelling between Athens and Clausthal by DAAD (Germany, Grant number 57068925) and IKY (Greece, Grant number 223) is gratefully acknowledged.

REFERENCES

[1] Schlapbach L, Zeuttel A. Hydrogen-storage materials for mobile applications, Nature 2001;414:353–8.
[2] Borodina TN, Grigoriev DO, Andreeva DV, Möhwald H, Shchukin DG. Polyelectrolyte multilayered nanofilms as a novel approach for the protection of hydrogen storage materials. ACS Appl Mater Interfaces 2009;1:996–1001.
[3] Kojima Y, Suzuki N. Hydrogen adsorption and desorption by potassium-doped superactivated carbon. Appl Phys Lett 2004;84:4113–5.
[4] Dillon AC, Jones KM, Bekkedahl TA, Kiang CH, Bethune DS, Heben MJ. Storage of hydrogen in single-walled carbon nanotubes. Nature 1997;386:377–9.
[5] Schlesinger HI, Brown HC, Finhold AE, Gilbreath JR, Hoekstra HR, Hyde EK. Sodium borohydride, its hydrolysis and its use as a reducing agent and in the generation of hydrogen. J Am Chem Soc 1953;75:215–9.
[6] Song Y. New perspectives on potential hydrogen storage materials using high pressure. Phys Chem Chem Phys 2013;15:14524–47.
[7] Di Pietro JP, Skolnik EG. Analysis of the sodium hydride-based hydrogen storage system being developed by PowerBall technologies, LLC. In: Proceedings of the 2000 U.S. DOE Hydrogen Program Review, San Ramon (California) and Golden (Colorado); 2000.
[8] Kojima Y, Suzuki K, Kawai Y. Hydrogen generation by hydrolysis reaction of magnesium hydride. J Mater Sci 2004;39:2227–9.
[9] Bogdanovic B, Schwickardi M. Ti-doped alkali metal aluminium hydrides as potential novel reversible hydrogen storage materials. J Alloys Compd 1997;253/254:1–9.
[10] Kojima Y, Kawai K, Kimbara M, Nakanishi H, Matsumoto S. Hydrogen generation by hydrolysis reaction of lithium borohydride. Int J Hydrogen Energy 2004;29:1213–7.
[11] Amendola SC, Sharp-Goldman SL, Janjua MS, Spencer NC, Kelly MT, Petill PJ, et al. An ultrasafe hydrogen generator: aqueous, alkaline borohydride solutions and Ru catalyst, J Power Sources 2000;85:186–9.
[12] Kojima Y, Kawai K. Hydrogen storage of metal nitride by a mechanochemical reaction. Chem Commun 2004:2210–1.
[13] Newson E, Haueter Th, Hottinger P, Von Roth F, Scherer GWH, Schucan ThH. Seasonal storage of hydrogen in stationary systems with liquid organic hydrides. Int J Hydrogen Energy 1998;23:905–9.
[14] Varin RA, Zbroniec L, Polanski M, Bystrzcki J. A review of recent advances on the effects of microstructural refinement and nano-catalytic additives on the hydrogen storage properties of metal and complex hydrides. Energies 2011;4:1–25.
[15] Sakintuna B, Lamari-Darkrim F, Hirscher M. Metal hydride materials for solid hydrogen storage: a review. Int J Hydrogen Energy 2007;32:1121–40.
[16] Wu C, Bai Y, Liu DX, Wu F, Pang ML, Yi BL. Ni–Co–B catalyst-promoted hydrogen generation by hydrolyzing $NaBH_4$ solution for in situ hydrogen supply of portable fuel cells. Catal Today 2011;170:33–9.
[17] Dahle S, Meuthen J, Schmidt A, Maus-Friedrichs W, Sourkouni G, Argirusis Chr. The influence of protecting polyelectrolyte layers on the temperature behavior of $NaBD_4$. RSC Adv 2014;4:2628–33.
[18] Kato S, Borgschulte A, Bielmann M, Züttel A. Interface reactions and stability of a hydride composite ($NaBH_4$ + MgH_2). Phys Chem Chem Phys 2012;14:8360–8.
[19] Borodina TN, Grigoriev D, Möhwald H, Shchukin D. Hydrogen storage materials protected by a polymer shell. J Mater Chem 2010;20:1452–6.
[20] Decher G, Hong JD, Schmitt J. Buildup of ultrathin multilayer films by a self-assembly process: III. Consecutively alternating adsorption of anionic and cationic polyelectrolytes on charged surfaces. Thin Solid Films 1992;210/211:831–5.
[21] Hendrickson DN, Hollander JM, Jolly WL. Core-electron binding energies for compounds of boron, carbon, and chromium. Inorg Chem 1970;9:612–5.
[22] Il'inchik EA, Volkov VV, Mazalov LN. X-ray photoelectron spectroscopy of boron compounds. J Struct Chem 2005;46:523–34.
[23] Hesse M, Meier H, Zeeh B. Spektroskopische Methoden in der organischen Chemie. 8th ed. Stuttgart: Thieme; 2011.
[24] ACD/C+H NMR predictors and database 2012. Toronto, ON, Canada: Advanced Chemistry Development, Inc.; 2012. www.acdlabs.com.
[25] Schutte CJH. The infra-red spectrum of thin films of sodium borohydride. Spectrochim Acta 1960;16:1054–9.
[26] Spartan '14. Irvine, CA: Wavefunction, Inc; 2013. available from: http://www.wavefun.com/.
[27] Becke AD. Density-functional exchange-energy approximation with correct asymptotic behavior. Phys Rev A 1988;38:3098–100.
[28] Perdew JP. Density-functional approximation for the correlation energy of the inhomogeneous electron gas. Phys Rev B 1986;33:8822–4.
[29] Frerichs M, Voigts F, Maus-Friedrichs W. Fundamental processes of aluminium corrosion studied under ultra high vacuum conditions. Appl Surf Sci 2006;253:950–8.
[30] Scofield JH. Hartree-Slater subshell photoionization cross-sections at 1254 and 1487 eV. J Electron Spectrosc Relat Phenom 1976;8:129–37.
[31] National Institute of Standards and Technology Electron Inelastic-Mean-Free-Path Database 1.1. http://www.nist.gov/srd/nist71.cfm. [accessed January 2014].
[32] Dobbins T, Kamineni V, Lvov Y. Nanoarchitecture of protective coatings for air sensitive metal hydrides. Mater Matters 2007;2:19–21.